Metallaboranes

DOI: 10.1002/anie.201208849

Boron Beyond the Icosahedral Barrier: A 16-Vertex Metallaborane**

*Dipak Kumar Roy, Shubhankar Kumar Bose, R. S. Anju, Bijan Mondal, V. Ramkumar, and Sundargopal Ghosh**

Dedicated to Professor Thomas P. Fehlner on the occasion of his 75th birthday

The development of polyhedron-expansion chemistry by Hawthorne and co-workers[1] pioneered the way to the synthesis of large metallacarboranes.[2,3] Since then, supraicosahedral clusters have been actively studied both experimentally[2–4] and computationally.[5–7] However, advances have been slow. Although the first 13-vertex metallacarborane was described over 40 years ago,[1] there are only about one hundred such compounds currently known.[2–4,8] In addition, only a handful of 14- and 15-vertex metallacarboranes have been reported (Figure 1)[4,9–12] and no examples of species containing 16 or more vertices in the polyhedron. This is unfortunate because several of the current applications of boron-cluster compounds, for example, as "least-coordinating anions",[13] electronics, ceramics, polymers, and nanomaterials, and in immunodiagnosis[2] and boron-neutron-capture therapy,[14] would benefit from higher nuclearity clusters containing larger numbers of boron atoms.

The computational study of boranes $[B_nH_n]^{2-}$ with $n > 12$ shows valuable structural tendencies. Brown and Lipscomb[5a] showed that for deltahedral structures $[B_nH_n]^{2-}$ with $n = 13$–24, the number of degree-six vertices increases with increasing n. This high-degree vertex of supraicosahedral geometry can be effectively occupied by transition-metal atoms or fragments.[3,4,15,16] Calculations further show that a heavy transition metal with more diffused orbitals is favored over a light transition metal in the formation of supraicosahedral geometry.[17] However, later studies[6a] suggest that $[B_nH_n]^{2-}$ with $n \geq 16$ have energetically accessible alternative structures that are not fully triangulated but progressively more favorable.

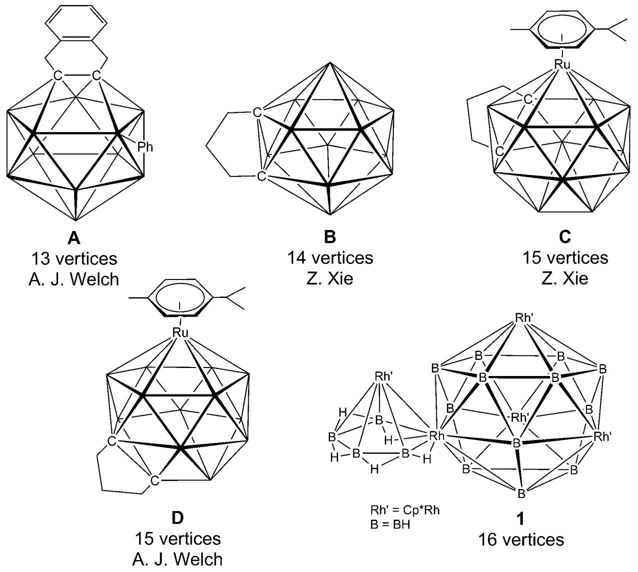

A
13 vertices
A. J. Welch

B
14 vertices
Z. Xie

C
15 vertices
Z. Xie

D
15 vertices
A. J. Welch

Rh' = Cp*Rh
B = BH

1
16 vertices

Figure 1. Earlier examples of supraicosahedral clusters with relatively high numbers of vertices (**A**–**D**) compared to the new 16-vertex rhodaborane **1**. **A**[4a]: 13-vertex carborane. **B**[11]: 14-vertex carborane. **C**[12] and **D**[4b]: 15-vertex ruthenacarboranes. **1**: 16-vertex rhodaborane $[(Cp^*Rh)_3B_{12}H_{12}Rh\ \{Cp^*RhB_4H_9\}]$.

Among the hundreds of metallaboranes and their derivatives reported by Fehlner and co-workers,[18] Kennedy,[19] and other groups,[20–22] only a few mono- or dimetallaboranes with 12 vertices[23] are known and none with more vertices. The lack of larger metallaboranes led us to renewed experimental efforts, and we recently reported the synthesis and structural characterization of dirhodium analogues of $[B_8H_{12}]$ and $[B_{10}H_{14}]$.[24] We now report an extension of these studies, which resulted in the isolation and characterization of the first 16-vertex *closo* metallaborane $[(Cp^*Rh)_3B_{12}H_{12}Rh\{Cp^*RhB_4H_9\}]$ (**1**, $Cp^* = \eta^5\text{-}C_5Me_5$). With its geometry based on a supraicosahedral framework, it provides a carbon-free example, thus demonstrating an additional structure type.

With regard to systematic cluster expansion, the most versatile metal is rhenium, and known Re_2B_n frameworks with $n = 4$–10.[23a] Fewer compounds are known with ruthenium[23b] and rhodium,[25] but use of a large excess of $BH_3{\cdot}THF$ and harsh conditions enables the isolation of 16-vertex rhodaborane **1** as a moderately stable yellow crystalline solid. The identity of **1** was confirmed by multinuclear NMR spectroscopy, elemental analysis, infrared spectroscopy, and X-ray structural analysis (Figure 2).[26] The cage of **1** has a 16-vertex polyhedron geometry with a degree-six Rh atom bound to a hexagonal B_6 belt (B1-B6), below which is an

---

[*] D. K. Roy, Dr. S. K. Bose, R. S. Anju, B. Mondal, V. Ramkumar, Prof. S. Ghosh
Department of Chemistry, Indian Institute of Technology Madras
Chennai, 600 036 (India)
E-mail: sghosh@iitm.ac.in

[**] This work was supported by the Department of Science and Technology, DST (Project No. SR/SI/IC-13/2011), New Delhi, India. Computational facilities from the IIT Madras computer center are gratefully acknowledged. D.K.R. is grateful to Council of Scientific and Industrial Research (CSIR), New Delhi, India, for Research Fellowship. We also thank the Center for Environmental Science and Technology, University of Notre Dame, for the mass analysis, supported by the NSF under CHE-0741793.

Supporting information for this article (including details of experimental and computational studies, and the crystal data for compounds **1** and **2**) is available on the WWW under http://dx.doi.org/10.1002/anie.201208849.

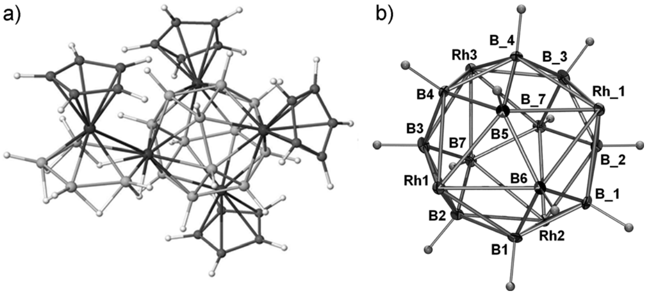

Figure 2. Molecular structure of **1** (50% probability ellipsoids). a) Complete structure of **1**. b) Core geometry of **1** without exopolyhedral unit. Selected bond lengths [Å] and angles [°]: Rh2–Rh4: 2.8754(6), Rh2–B1 2.234(4), Rh2–B7 2.258(4), Rh2–B_7 2.350(5), B5–B4 1.779(6), Rh3–B7 2.214(4), Rh3–B4 2.220(4); B6-B1-B_1 59.84(16), B_1-B1-B2 119.79(18), B6-B1-Rh1 65.99(19), B6-B1-Rh2 119.1(2), Rh1-B1-Rh2 124.62(19).

antiprismatic Rh_3B_3 belt (Rh_1-B_4). Below this, in turn, sits the B_2-B_3-B_7 trigonal unit. An interesting feature of this cluster core is the presence of an exopolyhedral $\{Cp^*RhB_4H_9\}$ anchored to one of the rhodium atoms in the Rh_3B_3 belt through η^5 bonding mode. Ignoring the *exo*-$\{Cp^*RhB_4H_9\}$ moiety, the metallaborane **1** has approximate C_s symmetry about the plane passing through Rh1, B_1, B_2, and Rh3. All the polyhedral faces in the cage of **1** are triangulated and all the B atoms are five-connected. Interestingly, all the Rh atoms are six-connected, consistent with the theoretical results, thus suggesting that metal atoms with relatively diffuse frontier orbitals tend to occupy the degree-six site(s) (see above).[3,4,15,16]

The total number of triangular faces in the core structure of **1** is 28, and so it can be called a icosioctahedron (or 28-hedron). This geometry is the same as that predicted for $[B_{16}H_{16}]^{2-}$ by theoretical calculations.[5a] The most interesting features of this structure are the coplanar B_6 bonding face and the chair conformation of the Rh_3B_3 bonding face (e.g., Rh_1-B_1-Rh2-B7-Rh3-B_4; Figure 2). The Rh1-B_6(centroid) distance (1.293 Å) and Rh3-B_6(centroid) distance (1.303 Å) are smaller than that in 14-vertex metallacarborane 2,13-$(CH_2)_3$-1-(*p*-cymene)-1,2,13-$RuC_2B_{11}H_{11}$ (1.46 Å).[12] The average distance between Rh and boron atoms in the cage (2.224 Å) is comparable to that in 1,4-$(CH_2)_3$-7-(*p*-cymene)-7,1,4-$RuC_2B_{12}H_{12}$ (2.247(3) Å).[12] The B–B bond distances in **1** follow the tendencies already established for supraicosahedral boron clusters.[3] The unique structural feature of **1** is a novel bonding approach of the exopolyhedral fragment to one of the rhodium atom (Rh2). The metal center (Rh2) is directly bound to the adjacent rhodium and two boron atoms of the exopolyhedral fragment (Rh2–Rh4: 2.8754(6) and Rh2–B8: 2.342(5) Å). In addition, the metal center also interacts with the *exo*-$\{Cp^*RhB_4H_9\}$ through an "agostic-like" Rh–H–B bond (Rh–H: 1.78(5) Å). Thus, the description Rh-η^5-$\{Cp^*RhB_4H_9\}$ can be used to exemplify this novel bonding mode. The results of molecular orbital calculations at the B3LYP level of theory suggest the same bonding situation for cluster **1** (see Figure S5 in the Supporting Information).

The ^{11}B NMR spectrum of **1** indicates a higher symmetry of the compound than is suggested by its solid-state structure. There are only four resonances between $\delta = 37$ and 5 ppm in the $^{11}B\{^1H\}$ NMR spectrum, with relative integrals of 6:6:2:2 (from high frequency to low frequency). This may be due to either fluxionality of cluster structure or inadvertent coincidence. Because the former reason is less likely, we suggest that both resonances of integral 6 result from a $2+2+1+1$ coincidence. All boron atoms of the 16-vertex cage are five-connected and coordinated to three other boron and two rhodium atoms, thus giving each an environment analogous to the apical atom in a *nido*-B_4Rh_2 pentagonal pyramid. With such similar coordination environments, the two resonances of the twelve cage boron atoms differ only because of the exopolyhedral substituent. Thus, one signal with intensity 6 belongs to the belt of boron atoms adjacent to the substituent, and the other signal with intensity 6 to the other belt of boron atoms. The signals with intensity 2 are then assigned to the exopolyhedral cluster substituent. The apparent C_s symmetry in solution is thus explained. The $^{11}B\{^1H\}$/$^{11}B\{^1H\}$ COSY spectrum is also consistent with these assignments. In the ^1H NMR spectrum, a single resonance for the three Cp* protons associated with the rhodium atoms of the 16-vertex cage appear at $\delta = 1.67$ ppm, while the exopolyhedral Cp* protons appear at $\delta = 1.70$ ppm. In addition to the resonances of BH terminal protons, the ^1H NMR spectrum shows three broad resonances at $\delta = -2.35$, -3.13, and -6.54 ppm. The latter resonance is assigned to the two Rh–H–B bridging hydrides. The resonances at $\delta = -2.35$ and -3.13 ppm are assigned to three B–H–B bridging protons of the exopolyhedral fragment $\{Cp^*RhB_4H_9\}$ and appear in 2:1 ratio, which is consistent with the structure. To test the fluxionality of **1**, variable-temperature $^1H\{^{11}B\}$ and $^{11}B\{^1H\}$ NMR analyses were undertaken. The high-field region of the $^1H\{^{11}B\}$ NMR spectrum shows no evidence of fluxionality. Also consistent with the NMR interpretation, the ^{11}B NMR chemical shifts of **1** show acceptable agreement with theoretical values, which were calculated by using the gauge-including atomic orbital density functional theory (GIAO-DFT) method at the B3LYP (SDD,6-31g*) level and referenced to $BF_3{\cdot}OEt_2$ (see Table S1 in the Supporting Information).

Compound **1** represents the first example of 16-vertex M_4B_{12} boron clusters. Its intriguing cage geometry can be viewed as a 16-vertex tetracapped truncated tetrahedron. The B_{12} core forms a truncated tetrahedron and the four rhodium atoms occupy the four hexagonal faces, thus generating the cage geometry of **1** (Figure 3). As a result, the polyhedral structure of **1** exhibits T_d symmetry, which is in contrast to the predictions of Schleyer and co-workers.[6a]

As noted by Brown and Lipscomb,[5a] closed polyhedra with 16, 19, and 22 atoms do not obey Wade's rule of $n+1$ skeletal electron pairs (seps).[27] Cluster **1** exhibits a 16-vertex deltahedral geometry that requires 17 seps, whereas formally only 16 seps are available. Also, a 16-vertex *closo* icosioctahedron geometry is exemplified by the discrete In_{16} cluster in the solid-state structure of $Na_7In_{11.8}$.[28]

Quantum-chemical calculations with DFT methods at the B3LYP (SDD, 6-31g*) level of theory have been used to provide further insight into the electronic structure and stability of the model cluster **1′** (Cp analogue of **1**). Selected DFT-optimized bond distances for the corresponding model

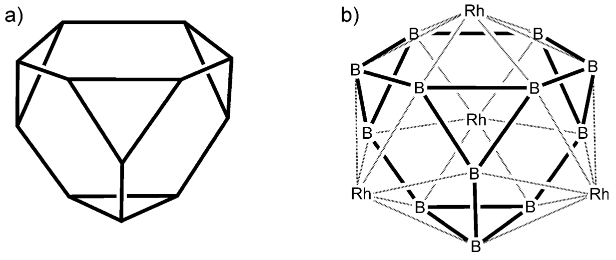

Figure 3. Visualization of the observed cage geometry of **1**. a) Truncated tetrahedron. b) Representation of a 16-vertex $[Cp^*_3Rh_4B_{12}H_{12}]$ framework in which four rhodium atoms cap the four hexagonal faces of a truncated tetrahedron.

cluster are given in Table S2 (see the Supporting Information). Satisfactory agreement is found between these computed bond lengths and those of the crystallographically characterized cluster. The DFT studies show the enhancement of thermodynamic stability of **1′** over *closo* borane $[B_{16}H_{16}]^{2-}$ and **1a**, a derivative of $[B_{16}H_{16}]^{2-}$ in which six-connected boron atoms are replaced by CpRh (see Figures S1–S3 in the Supporting Information). Indeed, a significant HOMO–LUMO energy gap of **1′** compared to **1a** and $[B_{16}H_{16}]^{2-}$ (ca. 3.5 vs. 1.28 eV and 0.99 eV, respectively; see Figure 4 and Table S3) is consistent with the theoretical findings of Lipscomb[5] and Jemmis.[7] Again, the three-dimensional aromatic character of **1′** is confirmed by a NICS(0) value of −16.1 ppm, which in turn plays a role in the stability of deltahedra. Figures S4 and S5 in the Supporting Information show significant bonding interaction (Weiberg bond indices (WBI) of 0.51) that corresponds to coupling of the Rh2 with B8 and B_8 atoms. Natural bond orbital (NBO) second-order perturbation energy analysis (31.15 and 31.77 kcal mol^{-1}) shows a donor–acceptor interaction between a filled B−H σ bond and an empty orbital on the Rh.

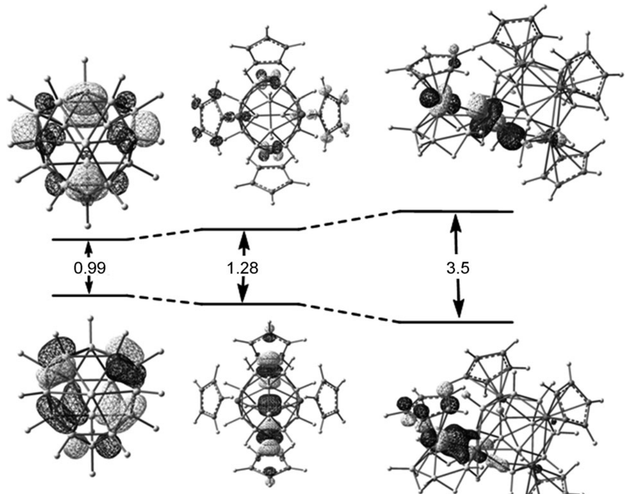

Figure 4. Molecular orbital diagrams for model complexes $[B_{16}H_{16}]^{2-}$, **1a**, and **1′**. **1a**: 16-vertex $[(CpRh)_4B_{12}H_{12}]^{2-}$ framework in which all four BH units at the hexagonal faces of $[B_{16}H_{16}]^{2-}$ are replaced by an isolobal CpRh fragment.

The general procedure used by Hawthorne and Dunks for the synthesis of larger clusters involves the opening of an *n*-vertex cage through reduction and insertion of a new vertex into the open face to form an $(n+1)$-vertex *closo* polyhedron.[29] Having a synthetic route to the 16-vertex cluster **1** established, we attempted to propose a possible pathway for the formation of **1**. A clue results from the isolation and characterization of $[(Cp^*Rh)_4B_6H_6]$ (**2**) as a by-product of the formation of **1**. The molecular structure of **2** displays a 10-vertex *closo* geometry,[30] with the six-connected Rh atom situated at the top of the Rh_3B_6 cage (Figure 5). If we exclude this Rh atom (Rh4), the Rh_3B_6 core of cluster **1** remains. Thus, the formation of **1** can be considered through a cluster expansion reaction of **2** by borane addition. However, attempts to insert BH fragments into **2** did not give the desired 16-vertex rhodaborane. Thus, **2** does not appear to be an actual intermediate in the formation of **1**. It is likely that **2** is formed from a *nido* or *arachno* cluster of the same nuclearity through the loss of hydrogen atoms. Thus, it is reasonable to consider that **2** possesses the composition (less hydrogen atoms) of a viable intermediate. In addition, **2** is notable in its own right. A number of 10-vertex *hypercloso* metallacarboranes as well as related *isocloso* metallaboranes are known,[17,31] however, the metal-rich *isocloso* rhodaborane **2** with four metal fragments is the first reported to have a 10-vertex geometry.

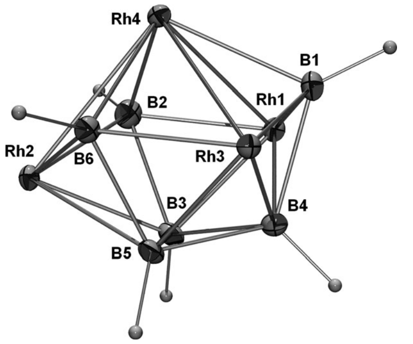

Figure 5. Molecular structure of **2** (50% probability ellipsoids). The Cp* ligands are excluded for clarity. Selected bond lengths [Å] and angles [°]: B1–B4 1.898(6), B1–Rh1 2.059(4), B3–Rh1 2.159(4), B5–B6 1.885(6), B6–Rh4 2.208(4), Rh1–Rh4 2.8013(4), Rh2–Rh4 2.7944(4); B4-B1-Rh1 66.35(16), B4-Rh3-B5 47.62(15), Rh3-Rh4-Rh1 82.372(10), Rh1-B1-Rh3 125.9(2).

In summary, this work describes the first isolation and structural characterization of a 16-vertex neutral cluster. Among the various ways that have been established for the formation of supraicosahedral carboranes and metallacarboranes, the general applicability of this procedure would be significant because, to our knowledge, it is the first example of the formation of supraicosahedral metallaborane through by M−X, B−H bond metathesis with neutral boranes. This observation provides a basis for the development of polyhedral boron clusters with even more vertices, thus allowing classes of boron clusters of large size and unique structures to be envisaged. Efforts to extend this study to such polyhedra are underway and will be reported in due course.

Experimental Section

Preparation of **1** and **2**: $[Cp^{*}RhCl_2]_2$ (0.07 g, 0.11 mmol) and toluene (12 mL) were added to a flame-dried Schlenk tube, and the resulting suspension was cooled to −78 °C. $LiBH_4{\cdot}THF$ (0.4 mL, 0.678 mmol) was added through a syringe, and the reaction mixture was allowed to slowly warm to room temperature and stirred for 1 h, resulting in an extremely air- and moisture-sensitive red-orange intermediate. The mixture was filtered and the filtrate concentrated. The intermediate was redissolved in toluene (15 mL) and thermolyzed with $BH_3{\cdot}THF$ (4.2 mL, 4.2 mmol) at 110 °C for 48 h. The solvent was removed in vacuo, and the residue was extracted into hexane and passed through Celite. After removal of the solvent in vacuo, the residue was subjected to chromatography using preparative silica gel TLC plates. Elution with a solvent mixture of hexane/CH_2Cl_2 = 90/10 (v/v) gave **1** (65 mg, 34 %) and **2** (23 mg, 21 %) a yellow and green solids, respectively.

1: MS (ESI$^+$) = 1248. Calculated mass for $^{12}C_{40}{}^{1}H_{81}{}^{11}B_{16}{}^{103}Rh_5$, 1249.5766, obsd, 1248.3260. ^{1}H NMR (400 MHz, [D$_6$]benzene): δ_H = 4.88 (partially collapsed quartet (pcq), 6 BH$_t$), 4.53 (pcq, 4 BH$_t$), 4.12 (pcq, 4 BH$_t$), 3.86 (pcq, 2 BH$_t$), 1.70 (s, 15 H; 1 Cp*), 1.67 (s, 45 H; 3 Cp*), −2.35 (br, 2 H; B-H-B), −3.13 (br, 1 H; B-H-B), −6.54 ppm (br, 2 H; Rh-H-B). ^{11}B NMR (128 MHz, [D$_6$]benzene): δ_B = 37.1 (d, J = 141 Hz, 6 B), 35.0 (d, J = 138 Hz, 6 B), 24.3 (d, J = 152 Hz, 2 B), 4.9 ppm (d, J = 132 Hz, 2 B). ^{13}C NMR (100 MHz, [D$_6$]benzene): δ_C = 103.5 ($C_5(CH_3)_5$), 101.3 ($C_5(CH_3)_5$), 9.6 ($C_5(CH_3)_5$), 9.1 ppm ($C_5(CH_3)_5$). IR (hexane): $\tilde{\nu}$ = 2475 w cm^{-1} (BH$_t$). Elemental analysis (%) calcd for $C_{40}H_{81}B_{16}Rh_5$: C, 38.45; H, 6.53. Found: C, 38.18; H, 6.33.

2: MS (ESI$^+$) = 1022. Calculated mass for $^{12}C_{40}{}^{1}H_{65}{}^{11}B_{6}{}^{103}Rh_4$, 1022.4337, obsd, 1022.1913. ^{1}H NMR (500 MHz, [D$_6$]benzene): δ_H = 3.26 (pcq, 2 BH$_t$), 2.65 (pcq, 4 BH$_t$), 1.78 (s, 30 H; 2 Cp*) 1.63 ppm (s, 30 H; 2 Cp*). ^{11}B NMR (160 MHz, [D$_6$]benzene): δ_B = 38.7 (d, 136 Hz, 4 B), 21.4 ppm (d, 144 Hz, 2 B). ^{13}C NMR (125 MHz, [D$_6$]benzene): δ_C = 103.8 ($C_5(CH_3)_5$), 9.63 ppm ($C_5(CH_3)_5$). IR (hexane): $\tilde{\nu}$ = 2538 w cm^{-1} (BH$_t$). Elemental analysis (%) calcd for $C_{40}H_{66}B_6Rh_4$: C, 46.94; H, 6.49. Found: C, 46.56; H, 6.19.

Received: November 4, 2012

Keywords: boron · cage compounds · metallaboranes · rhodium

---

[1] G. B. Dunks, M. M. McKown, M. F. Hawthorne, *J. Am. Chem. Soc.* **1971**, *93*, 2541–2543.

[2] a) A. K. Saxena, N. S. Hosmane, *Chem. Rev.* **1993**, *93*, 1081–1124; b) R. N. Grimes in *Comprehensive Organometallic Chemistry II*, *Vol. 1* (Eds.: E. W. Abel, F. G. A. Stone, G. Wilkinson), Pergamon, Oxford, **1995**, p. 373; c) R. N. Grimes, *Coord. Chem. Rev.* **2000**, *200–202*, 773–811.

[3] a) Z. Xie, *Coord. Chem. Rev.* **2002**, *231*, 23–46; b) J. Zhang, Z. Xie, *Chem. Asian J.* **2010**, *5*, 1742–1757; c) L. Deng, Z. Xie, *Coord. Chem. Rev.* **2007**, *251*, 2452–2476; d) Z. Xie, *Acc. Chem. Res.* **2003**, *36*, 1–9.

[4] a) A. Burke, D. Ellis, B. T. Giles, B. E. Hodson, S. A. Macgregor, G. M. Rosair, A. J. Welch, *Angew. Chem.* **2003**, *115*, 235–238; *Angew. Chem. Int. Ed.* **2003**, *42*, 225–228; b) R. D. McIntosh, D. Ellis, G. M. Rosair, A. J. Welch, *Angew. Chem.* **2006**, *118*, 4419–4422; *Angew. Chem. Int. Ed.* **2006**, *45*, 4313–4316.

[5] a) L. D. Brown, W. N. Lipscomb, *Inorg. Chem.* **1977**, *16*, 2989–2996; b) J. Bicerano, D. S. Marynick, W. N. Lipscomb, *Inorg. Chem.* **1978**, *17*, 3443–3453; c) W. N. Lipscomb, L. Massa, *Inorg. Chem.* **1992**, *31*, 2297–2299.

[6] a) P. v. R. Schleyer, K. Najafian, A. M. Mebel, *Inorg. Chem.* **1998**, *37*, 6765–6772; b) Z. X. Wang, P. v. R. Schleyer, *J. Am. Chem. Soc.* **2003**, *125*, 10484–10485.

[7] a) M. M. Balakrishnarajan, R. Hoffmann, P. D. Pancharatna, E. D. Jemmis, *Inorg. Chem.* **2003**, *42*, 4650–4659; b) E. D. Jemmis, M. M. Balakrishnarajan, P. D. Pancharatna, *Chem. Rev.* **2002**, *102*, 93–144; c) E. D. Jemmis, *J. Am. Chem. Soc.* **1982**, *104*, 7017–7020.

[8] a) N. S. Hosmane, J. A. Maguire in *Comprehensive Organometallic Chemistry III*, *Vol. 3* (Eds.: D. M. P. Mingos, R. H. Crabtree), Elsevier, Oxford, **2007**, p. 175; b) N. S. Hosmane, J. A. Maguire, *Eur. J. Inorg. Chem.* **2003**, 3989–3999.

[9] W. J. Evans, M. F. Hawthorne, *J. Chem. Soc. Chem. Commun.* **1974**, 38–39.

[10] W. M. Maxwell, R. Weiss, E. Sinn, R. N. Grimes, *J. Am. Chem. Soc.* **1977**, *99*, 4016–4029.

[11] L. Deng, H.-S. Chan, Z. Xie, *Angew. Chem.* **2005**, *117*, 2166–2169; *Angew. Chem. Int. Ed.* **2005**, *44*, 2128–2131.

[12] L. Deng, J. Zhang, H.-S. Chan, Z. Xie, *Angew. Chem.* **2006**, *118*, 4415–4419; *Angew. Chem. Int. Ed.* **2006**, *45*, 4309–4313.

[13] K. Shelly, C. A. Reed, Y. J. Lee, W. R. Scheidt, *J. Am. Chem. Soc.* **1986**, *108*, 3117–3118.

[14] L. F. Tietze, U. Griesbach, U. Bothe, H. Nakamura, Y. Yamamoto, *ChemBioChem* **2002**, *3*, 219–225.

[15] a) D. F. Dustin, G. B. Dunks, M. F. Hawthorne, *J. Am. Chem. Soc.* **1973**, *95*, 1109–1115; b) C. G. Salentine, M. F. Hawthorne, *J. Am. Chem. Soc.* **1975**, *97*, 426–428.

[16] A. R. Kudinov, D. S. Perekalin, S. S. Rynin, K. A. Lyssenko, G. V. Grintselev-Knyazev, P. V. Petrovskii, *Angew. Chem.* **2002**, *114*, 4286–4288; *Angew. Chem. Int. Ed.* **2002**, *41*, 4112–4114.

[17] O. Shameema, E. D. Jemmis, *Inorg. Chem.* **2009**, *48*, 7818–7827.

[18] a) T. P. Fehlner, *Organometallics* **2000**, *19*, 2643–2651; b) T. P. Fehlner, J.-F. Halet, J.-Y. Saillard, *Molecular Clusters. A Bridge to Solid-State Chemistry*, Cambridge University Press, Cambridge, **2007**; c) C. E. Housecroft in *Inorganometallic Chemistry* (Ed.: T. P. Fehlner), Plenum, New York, **1992**.

[19] a) J. D. Kennedy, *Prog. Inorg. Chem.* **1984**, *32*, 519–670; b) J. D. Kennedy, *Prog. Inorg. Chem.* **1986**, *34*, 211–434.

[20] N. N. Greenwood, I. M. Ward, *Chem. Soc. Rev.* **1974**, *3*, 231–271.

[21] L. Barton, D. K. Srivastava in *Comprehensive Organometallic Chemistry II*, *Vol. 1* (Eds.: E. W. Abel, F. G. A. Stone, G. Wilkinson), Pergamon, Oxford, **1995**.

[22] D. M. P. Mingos, D. J. Wales, *Introduction to Cluster Chemistry*, Prentice Hall, Englewood, NJ, **1990**.

[23] a) B. Le Guennic, H. Jiao, S. Kahlal, J.-Y. Saillard, J.-F. Halet, S. Ghosh, M. Shang, A. M. Beatty, A. L. Rheingold, T. P. Fehlner, *J. Am. Chem. Soc.* **2004**, *126*, 3203–3217; b) S. Ghosh, B. C. Noll, T. P. Fehlner, *Angew. Chem.* **2005**, *117*, 2976–2978; *Angew. Chem. Int. Ed.* **2005**, *44*, 2916–2918.

[24] D. K. Roy, S. K. Bose, R. S. Anju, V. Ramkumar, S. Ghosh, *Inorg. Chem.* **2012**, *51*, 10715–10722.

[25] a) X. Lei, M. Shang, T. P. Fehlner, *J. Am. Chem. Soc.* **1999**, *121*, 1275–1287; b) H. Yan, A. M. Beatty, T. P. Fehlner, *Angew. Chem.* **2001**, *113*, 4630–4633; *Angew. Chem. Int. Ed.* **2001**, *40*, 4498–4501.

[26] The crystal data for **1** and **2** were collected and integrated using a Bruker Axs kappa apex2 CCD diffractometer, with graphite monochromated Mo-Kα (λ = 0.71073 Å) radiation at 173 K. The structures were solved by heavy-atom methods using SHELXS-97 or SIR92 and refined using SHELXL-97. Crystal data for **1**: $C_{40}H_{81}B_{16}Rh_5$, M_r = 1249.56, orthorhombic space group *Pnnm*, a = 24.5282(15), b = 12.9676(7), c = 15.7330(9) Å, V = 5004.2(5) Å^3, Z = 4, ρ_{calcd} = 1.659 g cm^{-3}, μ = 1.644 mm^{-1}, $F(000)$ = 2504, R_1 = 0.0350, wR_2 = 0.0744, 5754 independent reflections [$2\theta \leq 56.48°$] and 345 parameters. Crystal data for **2**: $C_{40}H_{66}B_6Rh_4$, M_r = 1023.43, triclinic space group $P\bar{1}$, a = 9.9008(4), b = 11.2362(4), c = 19.4008(7) Å, α = 90.027(2), β = 92.599(2), γ = 108.663(2)°, V = 2042.44(13) Å^3, Z = 2, ρ_{calcd} = 1.664 g cm^{-3}, μ = 1.616 mm^{-1}, $F(000)$ = 1032, R_1 = 0.0316, wR_2 = 0.0795, 9750 independent reflections [$2\theta \leq 58.02°$] and 495

parameters. CCDC 901635 (**1**) and 901636 (**2**) contain the supplementary crystallographic data for this paper. These data can be obtained free of charge from The Cambridge Crystallographic Data Centre via www.ccdc.cam.ac.uk/data_request/cif.

[27] K. Wade, *Adv. Inorg. Chem. Radiochem.* **1976**, *18*, 1–66.

[28] S. C. Sevov, J. D. Corbett, *Inorg. Chem.* **1992**, *31*, 1895–1901.

[29] M. F. Hawthorne, G. B. Dunks, *Science* **1972**, *178*, 462–471.

[30] Compound **2** is related to the 10-vertex *isocloso* geometry, which is based on a 10-vertex *closo* bicapped square antiprism and obtained through a diamond-square-diamond (DSD) rearrangement. The six-membered open-face Rh_3B_3 (Rh1-B1-Rh3-B6-Rh2-B2), which is coordinated by the unique Rh atom, has an almost ideal chair conformation.

[31] J. Bould, N. N. Greenwood, J. D. Kennedy, W. S. McDonald, *J. Chem. Soc. Chem. Commun.* **1982**, 465–467.